

Calibrating A Spectrometer Via Global Bayesian Optimization on a Reference Setup

8241S

May 16, 2022

Abstract

In this investigation we attempt to create and test a robust software package, with the goal to provide calibration for a spectrometer, to be used for exoplanet surveying looking for Earth-like planets in HARPS. The proposed technique relies on a custom optical setup, used to provide reference light, and the software package to be developed, based of Global Bayesian Optimization. The complexity of the algorithms involved, however, proved to require a lot more investigation into optimizing differnt aspects of the process, with no successful example on test simulations. Troughout the investigation, however, a custom numerical integration technique was employed and given the large set of possible adjustments to be made to the algorithm used, it is not clear if it is suitable for the problem.

1 Introduction and Theoretical Background

1.1 The Problem

Doppler Method for Exoplanet Survey

One of the techniques used for exoplanet surveying is the so-called Doppler Method. It relies on the gravitational effect of the planet to be detected on the star, to which it is bound. The elliptical trajectory of the planets' orbit causes the parent star to also orbit around their common centre of

mass. This, in turn, alters the relative speed of the star to the Earth, which can be detected via movement of spectral lines of known wavelength, most commonly hydrogen lines. The data can be broken down in frequency to separate different planets' effect on the parent star. The result is indicative of the properties of the planets in that system in terms of mass and orbit radius and shape. The Doppler Method has been successfully employed in the search of planets, very close to their parent star or of large mass, comparable to that of Jupiter [6]. This process, however, requires great sensitivity for Earth-like planets, which is why new generation infrastructure, such as HARPS are constructed, relying on much more accurate spectrum observations.

The Doppler Effect.

To demonstrate the requirements on the spectrum measurement we discuss a simplified 2-body system of star and planet of mass ratio η . Thus we calculate that for observations in the orbital plane and for a circular orbit, the unitless doppler shift we expect is:

$$\frac{\Delta\lambda}{\lambda} \approx -\frac{v_1}{c} \sqrt{\frac{\eta^2}{(1+\eta)^3}} \quad (1)$$

Given the orbital speed of the planet, we expect for an Earth-like planet, a value of the order of $v_1 \approx 10^{-4}c$, $\eta \approx 10^{-6}$, thus giving the requirement to observe deviations of wavelength of the order of 1 part in 10^{10} .

Accuracy Requirements For Survey

As shown, surveys for Earth-like exoplanets via the Doppler Method, require extreme precision out of the spectrometers used, far exceeding the resolving power of spectrometers used today. This project considers the HARPS instrument, with spectral resolution $R = 115'000$. However, observations can still be made through long exposures, wherein the spectra observed have a sufficient variation that if a histogram is constructed from neighbouring pixels as well, and probability distribution functions fitted, small variations to the mean of that, distribution, representing the unmodulated spectral line, can be observed even at a precision level, orders of magnitude greater than the resolving power of the instrument. This however requires precise knowledge of the instrument used.

In particular, such spectrometers use CCD's with finite pixel sizes and sometimes defects in the precise position of the center of the pixels on the

CCD. Thus in order to achieve the required precision, these positions in the spectrum need to be determined. This leads to the need for robust and precise calibration methods.

An option proposed for determining the pixel positions of a CCD are so-called astro-combs [5], used to inject light of known spectrum, which is to be compared to the observed data from the spectrometer. The light is generated with very precise spectrum features, which are also quite narrow, made such through the use of Fabry-Perot cavities and custom hardware overall. This yields precision of 1 part in $\approx 10^9$, and is also an extremely expensive methodology. The goal of this investigation is to assess the viability of different, more affordable approaches.

1.2 Bayesian Optimization Technique

Achieving the required calibration precision, without using expensive hardware is generally a tall order. This investigation's proposed method for circumventing the need for astro-combs involves a more software-heavy approach. In detail, it involves injecting broadband light from a source of known properties, such as a tungsten lamp, through a Michelson Interferometer, into the spectrometer. This allows interference features to be introduced into the light, allowing for a varied spectrum.

Calibration is then performed by making intensity measurements, and comparing them to a model of the pixel positions, which is to be fitted to the observed light. The fitting is to be performed via a global optimization of the parameters, characterizing the model used, via Bayesian Optimization.

This method is well suited to the problem as it is developed for maximization of functions, which are expensive to evaluate, as model determination is in this case. The process follows an algorithm for optimization, described below.

Summary of Bayesian Optimization. [4]

1. Model Determination. The first step is to determine an appropriate model and parametrization, along with parameter space, for example given central positions of pixels \mathbf{x} , on a CCD, which are unperturbed, a model would take the form of: $f(\mathbf{x}, \mathbf{params}) \rightarrow \mathbf{y}$,

thus updating the estimates to the vector \mathbf{y} . Here a decision of the type of model to be used is important, since the Bayesian Optimization algorithm is unsuited for large-dimensional parameter sets, so simplifying the number of dimensions of this space is both computationally beneficial and a requirement for successful execution.

2. Set up. The algorithm requires an objective function, which is to be minimized, for example the $\chi^2 = \sum_i \frac{(E_i - O_i)^2}{E_i}$ value for the model for a given parameter set. It also requires a Gaussian Process $\mathcal{GP} = \mathcal{N}(\mu(x), k(x, x'))$, with $\mu(x)$ acting as the current best fit to the model (prior), while the kernel $k(x, x')$ acting as a covariance matrix, encapsulating the properties we need to capture. On this step we need to choose appropriate type of kernel, which would capture the desired behaviour of the model in question.
3. Iterative Step. On each step the algorithm uses the current values of μ, k , derived from observations so-far and uses an acquisition function on a random choice of function from \mathcal{GP} , taking the process and determining the next point in parameter space to be observed. This is used to construct a posterior distribution, to be used as the next step's prior. Here appropriate choice of acquisition function has to be made. There are a number of choices with different qualities.

This step also involves an improvement of the optimization of the hyperparameters of the problem, for example, the parameters used to define the kernel, such as length-scale σ for an Radial Basis Function kernel $k(x, x') = \exp\left(-\frac{\|x - x'\|^2}{2\sigma^2}\right)$, commonly used in this process. This is done in order to improve the estimates of $\mu(x)$ in following steps.

4. Finalizing. After a preset number of steps, the algorithm halts and its determined values can be recovered, in order to be used.
-

2 Process and Challenges

2.1 Modelling of the required function and set up

In order to assess the viability of the method proposed we need a simulation of the setup that is to be used in the actual instrument. To that end, we

introduce two factors, which contribute to the misalignment of pixels: Randomness and correlation. We produce a vector, which is to be found, of the deviation from the proposed centre via a normal random number generator, and we then correlate neighbouring pixel deviations spatially. The result is illustrated in Fig. 1.

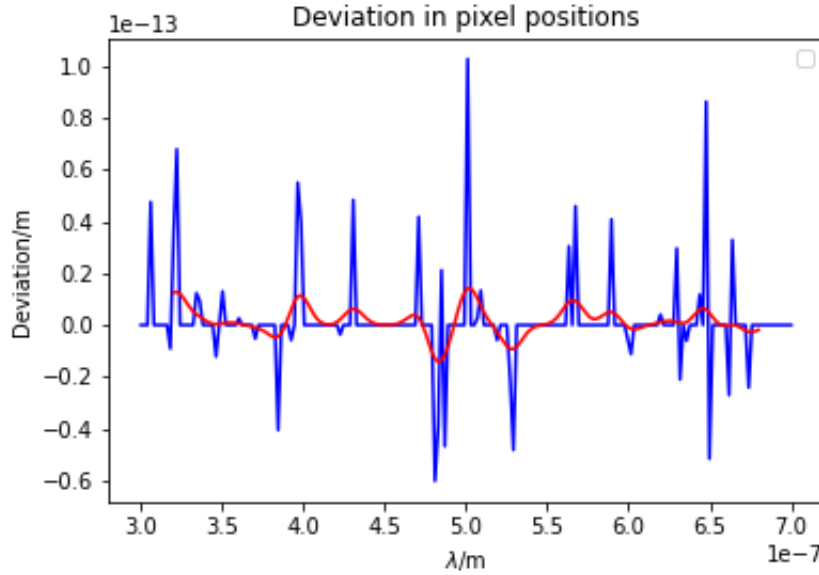


Figure 1: Simulated deviation in pixel positions, produced to be reproduced with a model. Here for simplicity we use 200 pixels and use correlation length of 1 pixel. In reality these can be included as hyperparameters in a more complex model.

The setup for the procedure then requires an appropriate model, which perturbs the pixel positions, The choice of parametrization is very important here as it determines the ability of algorithm to converge reliably. As such there are several possible choices, which were attempted in the course of the investigation. In all cases, given computational constraints, and the inability of the process to function with a large number of parameters, we resorted to a small number of parameters at leading order.

$$\lambda = f(\lambda_0) = \lambda_0 + a + b\lambda_0 + c\lambda^2 + d\lambda^3 + \dots \quad (2)$$

$$\lambda = f(\lambda_0) = \lambda_0 + a_0 + \sum_{n=1} a_n \cos(nk_0\lambda_0) + b_n \sin(nk_0\lambda_0) \quad (3)$$

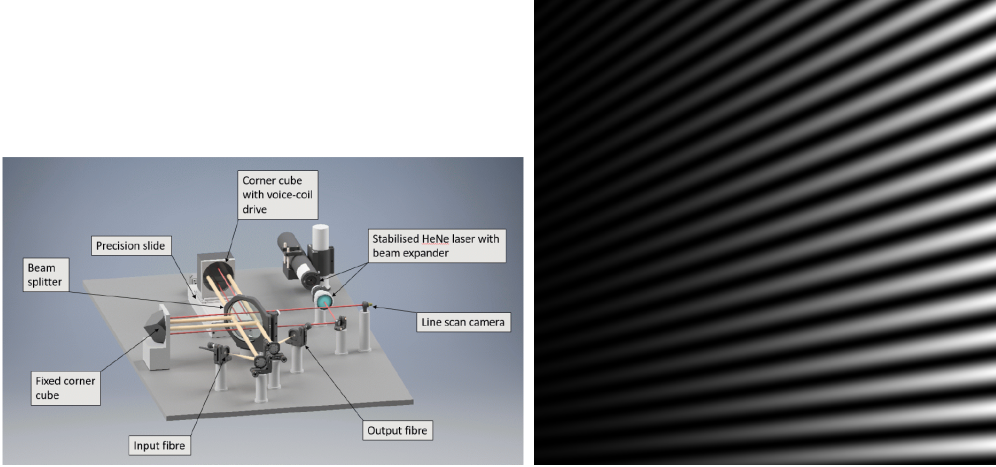
Given this we have models, which can be optimized, and it is then necessary to select parameter space boundaries. Through running the algorithm, developed, it became clear that real challenges to the procedure were presented when too large or too small spaces were chosen. In the former case, the algorithm will not explore the region of parameters we were interested in (Here the parameter boundaries were of the order of $10^2, 10^3$ of the actual parameter values used for testing purposes). In the latter case, it is obvious that the exploratory space needs to be greater than the actual values, which are to be approached. Thus it was concluded that convergence of the algorithm in a suitable time is only possible given that boundaries were preset to around 10 times the expected outcomes.

The next step of producing a working algorithm involves the choice of the so-called objective function. This is utilized by the process to assess the model accuracy to observation. As such we utilized the proposed hardware setup for calibration, which we simulated to deduce a global goodness-of-fit. Observations consist of simulating the black-body, intensity-normalized spectrum given off by a tungsten lamp. This is then passed through a Michelson interferometer, which has its optical path difference (OPD) calibrated to a satisfactory level of accuracy by through the use of a reference HeNe Laser and a long delay line [1]. This allowed, as seen on Fig.2 to produce spectra of varying intensity, resulting in a more pronounced change to the error function on deviation.

2.2 Challenges with evaluation of the objective function

The observational step, required to determine the goodness-of-fit at each step proved to be computationally challenging for a variety of reasons. First, each observation will involve computation of a matrix of the order of 10^9 10^{10} elements. This would be a manageable task, however the setup as described involves a lot of sources of uncertainty, for example, the temperature of the tungsten lamp used in practice. Black-body spectra are sensitive to temperature, and so changes in that parameter would involve a substantial change to

Figure 2: The proposed interferometer setup and an expected observation.



the expected, therefore modelled spectrum function and so prove the methodology hard to use.

A technique, we attempted to employ to remedy such sources is a custom numerical integration, targeted at integrals of the type

$$\int_0^{\infty} f(x)dx \quad (4)$$

wherein the integrand has a single pronounced maximum. Specifically in this case, we require for \mathcal{B} , being the normalized black-body spectrum for temperature T , modulated by $\cos(2\pi\frac{x}{\lambda})^2$, from the interferometer, and N is a the temperature normal distribution.

$$f(T) = \mathcal{B}(T, \lambda, x) \mathcal{N}(T_{\mu}, T_{\sigma}) \quad (5)$$

The integration technique.

The problem presented with integrals of type in Eq.(4) are related to the sampling required to calculate numerical integrals, used by all methods. Most commonly sampling is done linearly, but the upper limit of the integral, requires consideration of the asymptotic behaviour as $x \rightarrow \infty$, but also requires that sampling be sufficiently dense within the peak of the function, so that its behaviour is accurately captured there. As such linear or even logarithmic sampling is not optional. The proposed

method involves fitting a normal distribution as closely as possible to the integrand, and using it to sample that integrand, with sampling being dense within the peak of the function and sparse at the large values off the integral, where contributions are small, matching the requirements outlined above. The integral is hence calculated via a common methodology for numerical integration from samples, here we employ Simpson's technique, given its ease of use and relative accuracy. To allow for control over the method we also employ a multiplicative parameter of the standard deviation of the fitted Gaussian, to investigate possible changes to the method accuracy with the spread of the samples. We observed optimal performance around the $10^1, 10^3$ range as displayed by Fig.3. We also observe that for low values of the multiplier the integral value is reduced from the true value (the plateau), whereas large multiplier values yield significant errors. Thus we get the preferred multiplier of $\approx 10^2$.

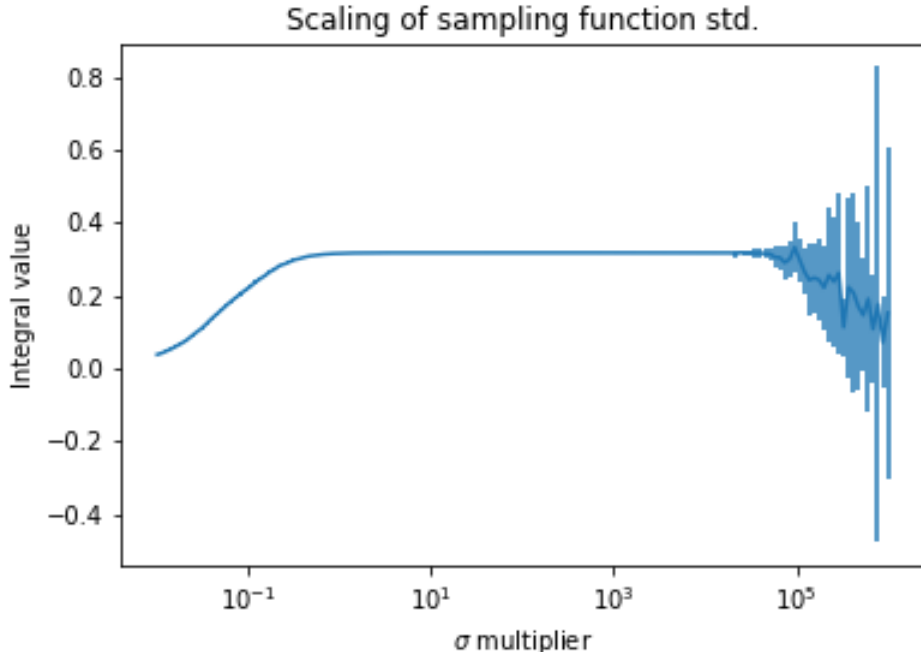


Figure 3: A display of the effect of the multiplicative parameter on the value of an integral of black-body spectra. Here each integration required 10^6 sample points

The next step of the algorithm involves the choice of kernel and its param-

eters, required for the purposes of the model, which we need, to be passed to the internal Gaussian Process Regressor. Here the choice rests on assumptions about the function in question, such as its differentiability, its periodicity, its length scales. As we make no assumptions beside those already in place by fixing the form of the model, we use is commonly used, the Matérn kernel [4]. To this we add a White Kernel, used to model noise, which we also later introduce in the observation. Both these kernels come equipped with a set of parameters, which are to be optimized by the internal gaussian process regressor used. These are as follows. The Matérn kernel comes with a length scale parameter and a ν parameter, the former encoding the dependence of parameter values on their immediate neighbourhood, the latter encoding the differentiability of the functions to be considered. While, given the information on the shape of function we consider, the length scale was varied less during the investigation, the ν parameter was varied between the 3 starting values of 0.5, 1.5, 2.5, which are ones, for which analytical, computationally light functions were implemented. The White Kernel comes with a noise-level parameter, which was given an initial value of 0. In all cases the Bayesian Optimization Process implements hyperparameter optimization (The 3 parameters of the kernel mentioned above), through a process in which the regressor assesses candidates for possible hyperparameters by evaluating the log-marginal-likelihood for the space given.

The last step is the choice of acquisition function number of iterations. For this investigation, we had the goal of attempting to show that the methodology is useful. To that end we chose 2 common acquisition functions to try: Expected Improvement [4], which is more robust, but is very costly to evaluate, and Upper Confidence Bound. The latter is relatively easy to evaluate and is known to be able to produce good results. Thus more often than not UCB was used, along with parameters which are fixed, which are used to balance the random exploration with guided exploitation of the algorithm.

2.3 Tests Performed

In order to test the viability of the models presented, various tests were performed on a simplified simulation, using an already developed implementation. [3] [2] These simulations used reduced pixel sizes (between 200 and 2000) and OPD spaces, in order to more efficiently investigate the effect of different aspects of the algorithm. To investigate the ability of the process to converge, tests with set parameters were performed, with 2, 3, 4 or 5 param-

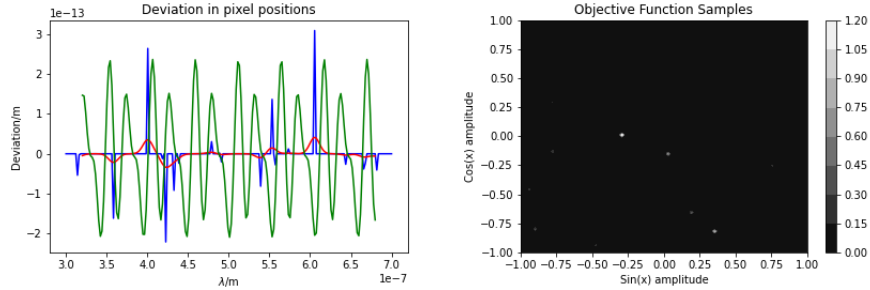


Figure 4: Tests performed in order to evaluate the objective function responsiveness and the model (red line is actual values, green line is the model) fit after 130 iterations.

eters in the model. As well as this, tests were performed with noisy inputs to the spectrum evaluations, varying the different levels of noise with respect to the signal input in the range of 10^{-1} , 10^{-5} , as well as varying sizes of the parameter spaces. These are values, which were used as they are commonly observed in processes, such as the optical measurements performed here.

The tests showed no reliable way to get a converging model. No test displays this. Further investigations into the parameter function, evaluated on parameter spaces revealed that the structure of the objective function is not suitable for the optimization algorithm, as shown in Fig. 4

Investigation was also attempted a number of times after developing the complete package. This, however, proved fruitless also since computation times for the simulation as a whole, generally speaking were found to be of the order of days. This presented a serious challenge to gathering quality data for assessment of the method.

3 Discussion

The failure to produce any reasonably convergent algorithm might indicate that this methodology is not optimal for the problem at hand. However such strong conclusion cannot be drawn from this investigation alone, given the time and resource constraints. It is possible that a greater amount of time needs to be allocated to parallelizing the software, built for the simulations, allowing for a much more comprehensive read of the possibilities. This, however, comes with its set of challenges, such as the difficulty of performing

that task and also there are limitations such as the floating point format used to pass to parallel systems. Another possibility is that the models attempted were not suitable for this test. A more in-depth analysis would be required to determine a better strategy for the calibration.

References

- [1] David F. Buscher, Roger C. Boysen, Roger Dace, Martin Fisher, Christopher A. Haniff, Eugene B. Seneta, Xiaowei Sun, Donald M. A. Wilson, and John S. Young. Design and testing of an innovative delay line for the MROI. In John D. Monnier, Markus Schöller, and William C. Danchi, editors, *Society of Photo-Optical Instrumentation Engineers (SPIE) Conference Series*, volume 6268 of *Society of Photo-Optical Instrumentation Engineers (SPIE) Conference Series*, page 62682I, June 2006.
- [2] The scikit-learn development team. David Cournapeau et al. Scikit-learn for python.
- [3] fmf. Bayesian optimization implementation for python using scikit-learn.
- [4] Peter I. Frazier. A tutorial on bayesian optimization, 2018.
- [5] Chih-Hao Li, Andrew J. Benedick, Peter Fendel, Alexander G. Glenday, Franz X. Kärtner, David F. Phillips, Dimitar Sasselov, Andrew Szentgyorgyi, and Ronald L. Walsworth. A laser frequency comb that enables radial velocity measurements with a precision of 1 cm s⁻¹. *Nature*, 452(7187):610–612, apr 2008.
- [6] Michel Mayor and Didier Queloz. A Jupiter-mass companion to a solar-type star. *Nature*, 378(6555):355–359, November 1995.